Fault complexity associated with the 14 August 2003 Mw6.2 Lefkada, Greece, aftershock sequence

Article *in* Acta Geophysica · October 2010

DOI: 10.2478/s11600-010-0009-6

CITATIONS
22

READS
171

2 authors:

Vassilios Karakostas
Aristotle University of Thessaloniki
175 PUBLICATIONS **3,156** CITATIONS

SEE PROFILE

Eleftheria Papadimitriou
Aristotle University of Thessaloniki
292 PUBLICATIONS **3,825** CITATIONS

SEE PROFILE

VERSITA

Acta Geophysica
DOI: 10.2478/s11600-010-0009-6

Fault Complexity Associated with the 14 August 2003 M_w6.2 Lefkada, Greece, Aftershock Sequence

Vassilios G. KARAKOSTAS and Eleftheria E. PAPADIMITRIOU

Department of Geophysics, University of Thessaloniki, Thessaloniki, Greece
e-mails: vkarak@geo.auth.gr, ritsa@geo.auth.gr

Abstract

The M_w6.2 Lefkada earthquake occurred on 14 August 2003 beneath the western coastline of Lefkada Island. The main shock was followed by an intense aftershock activity, which formed a narrow band extending over the western coast of the Island and the submarine area between Lefkada and Kefalonia Islands, whereas additional off fault aftershocks formed spatial clusters on the central and northwestern part of the Island. The aftershock spatial distribution revealed the activation of along-strike adjacent fault segment as well as of secondary faults close to the main rupture. The properties of the activated segments were illuminated by the precisely located aftershocks, fault plane solutions determination and the cross sections performed parallel and normal to their strike. The aftershock focal mechanisms exhibited mainly strike slip faulting throughout the activated area, although deviation of the dominant stress pattern is also observed. The results help to emphasize the importance of the identification of activated nearby fault segments possibly triggered by the main rupture. Because such segments are capable to produce moderate events causing appreciable damage, they should be viewed with caution in seismic hazard assessment in addition to the major regional faults.

Key words: aftershock sequence, complex faulting, Lefkada Island (Greece), 14 August 2003 Lefkada earthquake.

1. INTRODUCTION

The active deformation manifestation during a seismic excitation contributes to our understanding of both localized faulting properties and behavior of the seismicity associated or triggered by a main event. Motivation for such investigation is tempted for the 2003 Lefkada aftershock sequence, because of the fact that in addition to the activity taken place close to the main rupture, the seismic activity was expanded in a broader area and continued there for months. The main shock (M_w6.2) occurred on 14 August, exhibited a dextral strike-slip mechanism (strike = 18°, dip = 60°, slip = –175°, CMT solution) and is associated with a dextral strike slip fault which is located along the northwestern coastline of Lefkada Island (shown by a rectangle in Fig. 1). The properties of the seismic sequence were studied by the use of precise aftershock locations resulting from the recordings of a dense portable digital seismic network (Karakostas *et al.* 2004). Evidence is also presented by the same authors on the triggering of seismicity in the neighboring along-strike fault segment, due to the static stress changes from the main shock. The 2003

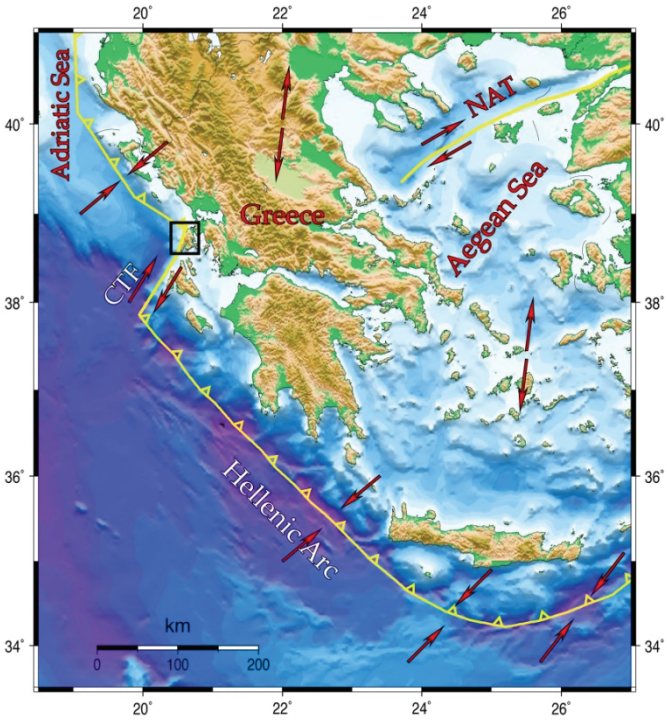

Fig. 1. The main geodynamic features of the broader Aegean region shown on a relief map. The active boundaries are shown as solid lines. The arrows indicate the approximate direction of relative plate motion. The study area is denoted by the square. NAT: North Aegean Trough, CTF: Cephalonia Transform Fault.

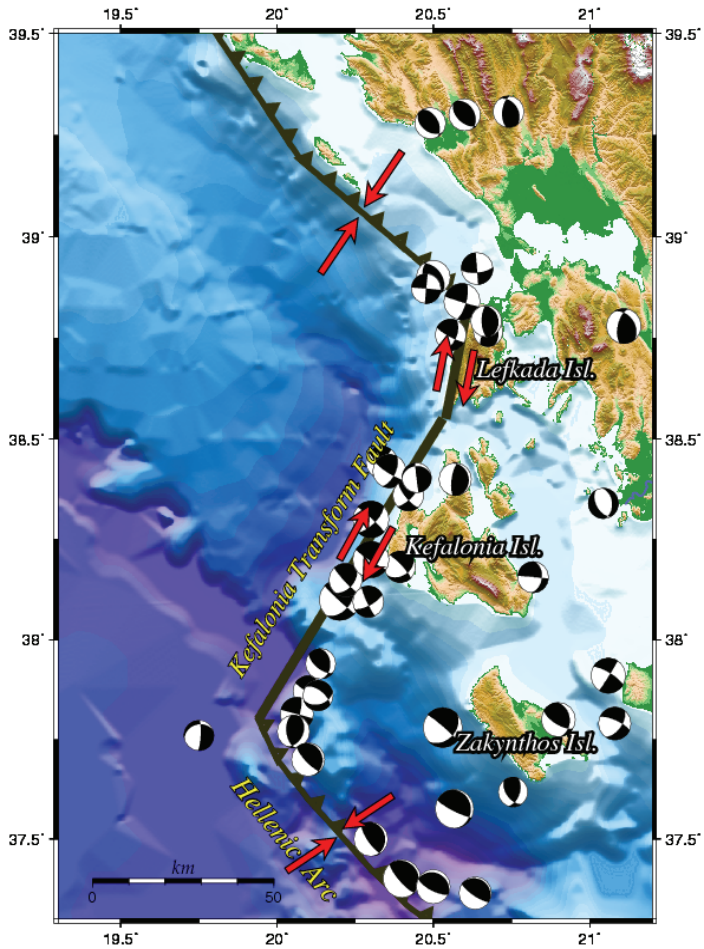

Fig. 2. Main active boundaries in the area of central Ionian Islands. The dextral strike slip Kefalonia and Lefkada fault segments are traced (consisting the Kefalonia Transform Fault System), the collision front to the north and the subduction front to the south. The most reliable available fault plane solutions of the strong earthquakes that occurred in the area in the last four decades are shown as lower hemisphere equal area projections.

Lefkada earthquake and its aftershocks illuminated for the first time the position of the causative fault which bounds the Island's western coastlines, which serves to emphasize the hazard associated with the largest earthquakes of this region.

Frequent strong ($M \geq 6.0$) earthquakes are known to have occurred in the study area (Fig. 2), which caused collapse of buildings, injuries and loss of life (Papazachos and Papazachou 2003). The northwestern part of the Island,

in particular, has experienced such events twice in the 20th century, in 1914 (M6.3) and in 1948 (M6.5), most probably associated with the same fault segment that activated in 2003. Furthermore, the macroseismic effects of the 1849 (M~6.4) earthquake also revealed the activation of this fault segment. Seismotectonic properties investigation, as detailed as possible, of this and related secondary fault segments, is thus become unambiguous for the future seismic hazard evaluation.

The 2003 seismic sequence has attracted the interest of the scientific community. Papadopoulos *et al*. (2003) estimated I_{max} = VIII in the city of Lefkada, and a range of intensities between V and VII for other parts of the Island, based on observations on landslides, rock falls, soil liquefaction and ground cracks. Field observations were accomplished and a preliminary microzonation map was established based on the liquefaction potential index for the city of Lefkada by Papathanassiou *et al*. (2005). It was suggested that the rupture process was dominated by two main events, one at the western coast of Lefkada Island and the other near the northwestern coast of the nearby Kefalonia Island (Zahradník *et al*. 2005, Benetatos *et al*. 2005). The source parameters of the main shock (shown as an asterisk in Fig. 3) were determined by Papadimitriou *et al*. (2006) using body-wave modeling, whereas a detailed slip distribution model is given by Benetatos *et al*. (2007), based on the double event interpretation.

The aftershock data used by Karakostas *et al.* (2004) run into tens of hundreds and cover the period 15-21 August 2003 (from the next day up to one week after the main shock occurrence). Although adequate in number, they turned to be inadequate in revealing details of the aftershock sequence complexity. Therefore, relocation and enrichment of the aftershock data set was performed by Karakostas (2008) for this purpose. It was evidenced that the aftershock activity was tightly confined on the main rupture and nearby secondary faults during the first twelve or more hours and then expanded southwestwards in a distance larger than 60 km.

The goal of this work is to investigate faulting complexity revealed from secondary structures that activated contemporaneously with the 2003 Lefkada main shock. In addition to the relocated aftershocks, fault plane solutions were determined for the purpose of the present study. Because the portable digital network was installed the day after the main shock occurrence, there are thousands of well-recorded aftershocks which can be used to infer stress orientations and make a study of the activated structures with a spatial resolution of 1 km, in both horizontal and vertical coordinates (Karakostas 2008).

The spatial distribution of the aftershock activity both onto and off fault revealed distinctive spatial clusters, which demonstrate the complex nature of the tectonics of this region. Although evidence for complex activity was

reported for other seismic sequences in Greece (e.g., Kozani sequence, Hatzfeld *et al.* 1997), documentary relative results are not available due probably to the lack of proper data. The quality and abundance of the data that are available for the purposes of the present study are expected to provide new insights into the regional seismotectonics and seismological aspects of such sequences.

2. SEISMOTECTONIC SETTING

The study area constitutes part of the Kefalonia transform fault system (CTF) which runs along the western coasts of Lefkada–Kefalonia Islands (Fig. 2). The system connects continental collision to the north with subduction to the south. Continental collision takes place between the Adriatic microplate and the mainland of Greece, a part of the Eurasian lithosphere. A belt of thrust faulting, with a NE-SW direction of the axis of maximum compression, runs along the eastern coastline of Adriatic Sea, and terminates just north of the Lefkada Island. The subduction of the eastern Mediterranean oceanic floor beneath the Aegean microplate, which starts south of Kefalonia Island, forms the Hellenic Arc (Papazachos and Comninakis 1971), which is the most prominent tectonic feature of the region. Seismic activity is very high throughout the arc where thrust faulting is also dominant.

The CTF is a major dextral strike slip fault system that accommodates frequent strong earthquakes, clustered in space and time possibly due to the stress transfer between adjacent fault segments (Papadimitriou 2002). The dextral strike-slip character of the CTF was first evidenced by Scordilis *et al*. (1985) and then supported further by Kiratzi and Langston (1991) and Papadimitriou (1993). It consists of two main segments, namely the Kefalonia and Lefkada segments (Papazachos *et al*. 1998, Louvari *et al*. 1999), that differ slightly in their strike and the magnitude of the maximum observed earthquake, which equals to 7.4 for Kefalonia and 6.7 for Lefkada segment (Fig. 2).

Historical information and instrumental data reveal that the disastrous earthquakes that occurred in Lefkada Island are all located along its western coastline, meaning that these events are associated with activation of the Lefkada fault segment. The investigation of the seismotectonic properties of this segment, by any data set that became available, is then of paramount importance for seismic hazard purposes.

3. SEISMICITY DATA

Following the main shock, a network of seven instruments was installed, with spacing between stations varying between 5 and 10 km (hexagons in Fig. 3a). The temporary installation greatly improved station coverage around

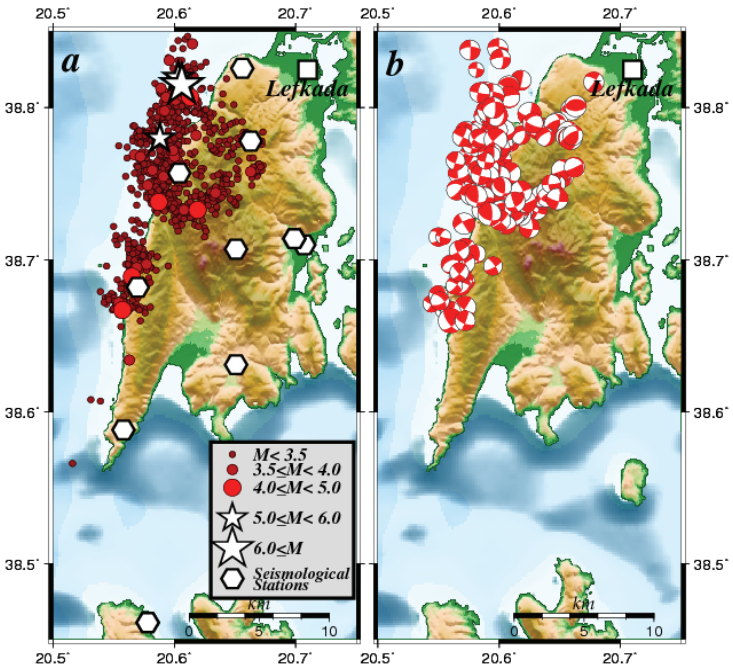

Fig. 3. The aftershock region showing (a) the epicenters of the events occurred from 14 August through 15 September 2003, with the main shock epicenter depicted as an asterisk, along with the positions of the seismological stations depicted as hexagons; and (b) aftershocks first motion focal mechanisms as lower hemisphere equal area projections, with the main shock focal mechanism shown by a distinctively bigger beach ball.

the activation area and provided valuable data. The sites were serviced daily during the first weeks and afterwards every three to four weeks, and the data were merged with the ones of the permanent station (located in the central mountainous area, Fig. 3a) being in operation in Lefkada Island. Exploitation of the data covering the first week after the main shock occurrence was done by Karakostas *et al*. (2004) who investigated the evolution of the seismic sequence and first defined the position of the causative fault as abutting the steep western coastline, while it was previously considered to be more offshore. The recorded aftershocks presented a complex pattern, clustering in groups separated by less active patches. This observation led us to seek for a detailed investigation of the activated structures that accommodated the seismic activity contemporaneously with the main rupture. For this purpose, in addition to the precisely located events, fault plane solutions for a large number of aftershocks were determined in the framework of the present study.

Aftershock locations

Although the temporary network stations provided valuable data for aftershock detection and location with high precision, the routine locations were improved by Karakostas (2008) who used the HYPOINVERSE computer program (Klein 2002). This relocation effort included more aftershock data, which cover the period of one month, and the calculation of new station delays specific to the aftershock zone. Repetitive iterations were performed to estimate the mean residuals for each seismological station, until obtaining values that were not changed by more than ±0.1 s, and were adopted as station corrections. This approach greatly reduced the number of events that were mislocated at or near zero depth and resulted to stable solutions with RMS ≤ 0.2 s.

Our aftershock dataset consists of 2644 well-located events (Fig. 3a). The aftershock depths range between ~2 and 13 km, the majority of them placed below 4 km. This is consistent with the findings for the seismogenic layer in other areas of the Greek territory, which is in general defined between 3 and 15 km. Spatially, the aftershocks consist of two primary cluster regions, one region near the main shock in the northern part of the aftershock zone, and the second one in the southern part, with a relatively aseismic region in between. In the northern cluster in turn, although the seismicity looks more diffuse, three subclusters can be demarcated. The main one is along the western coastline, where the main rupture was allocated (from Karakostas *et al*. 2004), with epicenters aligned in full agreement with main shock focal mechanism (strike = 18°, dip = 60°) as far as both fault orientation and expected width of the aftershock zone. Two more subclusters are specified, spaced to the northeast and southeast parts of the main cluster, which evidence the activation of secondary faults and the complex properties of the sequence.

Focal mechanisms

First-motion focal mechanisms were determined for all aftershocks with at least seven impulsive first motions. The mechanisms were determined using the FPFIT computer program (Reasenberg and Oppenheimer 1985). We obtained high to moderate quality solutions for one hundred and sixty earthquakes. These events had stable solutions with low polarity misfits and/or low azimuthal gap. The aftershock focal mechanisms are shown in Fig. 3b.

The aftershock focal mechanisms are mostly of dextral strike-slip faulting, compatible with the regional kinematic and dynamic model, as presented in the previous section. A low variance is indicative of heterogeneous stress conditions. Only a very few mechanisms indicate normal or reverse faulting, with some of them being positioned on the secondary activated structures.

4. SPATIAL DISTRIBUTION OF AFTERSHOCKS

The aftershocks that occurred from 15 August to 15 September 2003 form a complex spatial distribution. A space-time plot revealed that aftershock activity was confined close to the main shock epicenter during the first 12 hours and then expanded to the south-southwest, where it continued with a high rate for at least twenty days (Karakostas 2008). The expansion of the activity is considered to be triggered, since it coincides with a positive lobe of Coulomb stress changes due to the main shock slip (Karakostas *et al*. 2004). The occurrence of a moderate (M_w5.3) event in the southwestern most part of the activated region, almost three months afterwards, on 16 November 2003, provides more evidence on the possible triggering. The only change that can be seen from the space-time plot of aftershocks was the quick decay of aftershock activity located within 5 km of the northwestern edge of the distribution.

Most of the activity is concentrated along the western coast and to the east of the main rupture and, therefore, we seek for in this part rather than the whole activated area. The most dense clusters along the western coastline and to the east of the main rupture continued to be active for the interval of the four months covered by our data set, which comprises, in addition to the events located from the local network recordings, also those recorded by the regional national network and relocated by Karakostas (2008). In map view, the aftershocks form a 22-km long and 15-km wide zone in the northwestern part of the Island, separated by a 3-km distinct gap in the activity with an 11-km long dense cluster aligned along the central part of the western coastline.

To improve our understanding on how the spatial distribution relates with activated along strike or secondary active structures, the aftershock spatial distribution is examined on both strike-normal and strike-parallel cross sections. To detect possible spatial changes in the style of aftershock faulting, we show focal mechanisms that are grouped along with the hypocentral clustering. Figure 4 shows the four polygons (outlined in gray), which are set to encompass earthquake locations and fault plane solutions of the events constituting the respective four clusters. Continuous lines are the locations of strike parallel sections, whereas dashed lines the locations of strike normal sections.

Strike-parallel cross sections

To investigate aftershock distribution confined onto the main rupture, we show one cross section parallel to the strike of the main shock (Fig. 5a). The strike-parallel cross section includes the aftershocks above and to the south-southwest of the main shock hypocenter. Aftershock foci are mostly between

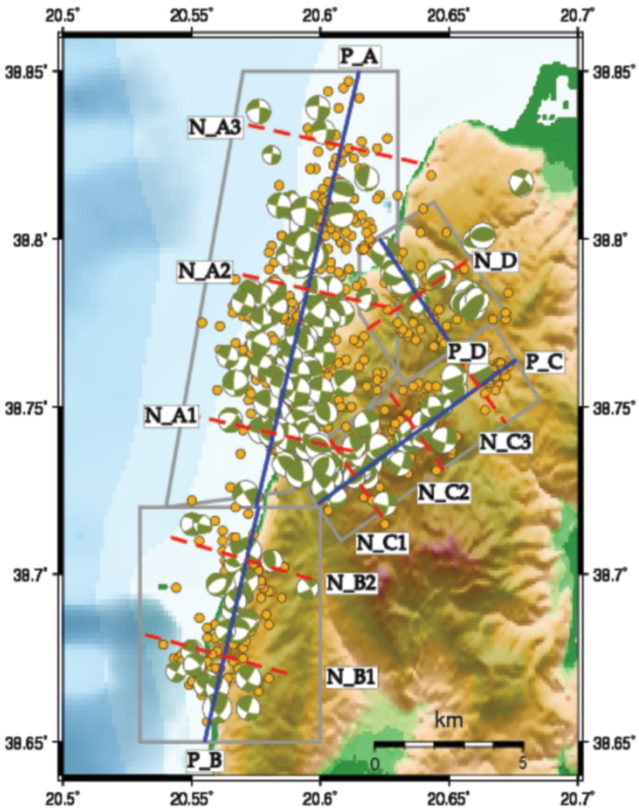

Fig. 4. Map of the study area where the epicenters and focal mechanisms are astricted within the limits of four polygons, which are sketched to encompass the four distinctive clusters. The thick lines indicate the surface position of the planes set for strike parallel cross sections (P_A for the main rupture, P_B for the western cluster, P_C for the central–eastern cluster and P_D for the northeastern cluster). The dashed lines indicate the surface position of the planes set for strike normal cross sections (denominated with a respective way). Colour version of this figure is available in electronic edition only.

4 and 12 km with very few being shallower or deeper. This distribution displays the unilateral character of the main rupture along with its dimensions, and became denser on some patches onto the rupture plane far from the main shock focus. This provides evidence for the coseismic slip distribution, which probably left the certain patches less affected during the main rupture.

Figure 6a exhibits the cross section that was accomplished in SSW-NNE direction, parallel to the long axis of polygon B (see Fig. 4), which encompasses the events of the south cluster. This cluster, which is distinctive in the map view, is considerably shallower than the other activity with most focal depths ranging between 2 and less than 8 km.

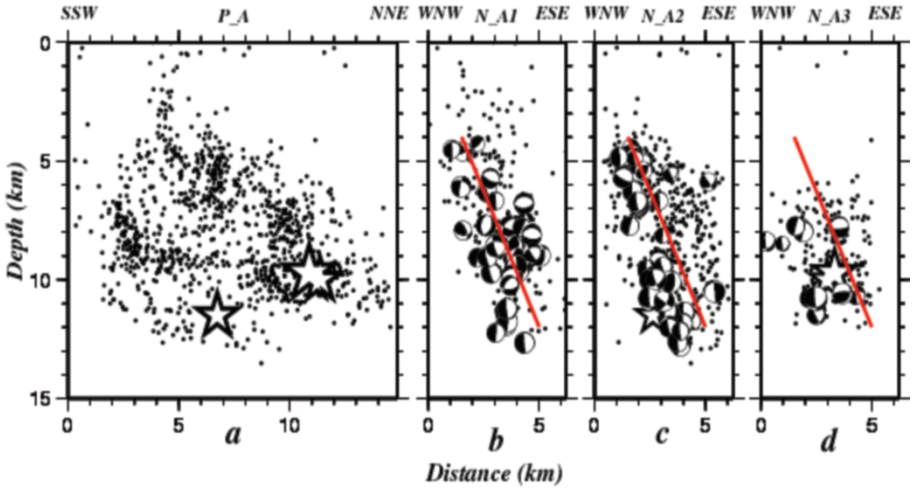

Fig. 5. Depth cross sections taken parallel (a) and normal (b, c, d) to the strike of the main rupture (for the positions of the cross sections, see Fig. 4). Strike normal cross sections are aligned perpendicular to strike parallel cross section and include events within 2.5 km of either sides of the cross-section plane. Stars depict the main shock and two larger ($M_w \geq 5.0$) aftershock foci. The focal mechanisms are shown as equal area projections of the front hemisphere.

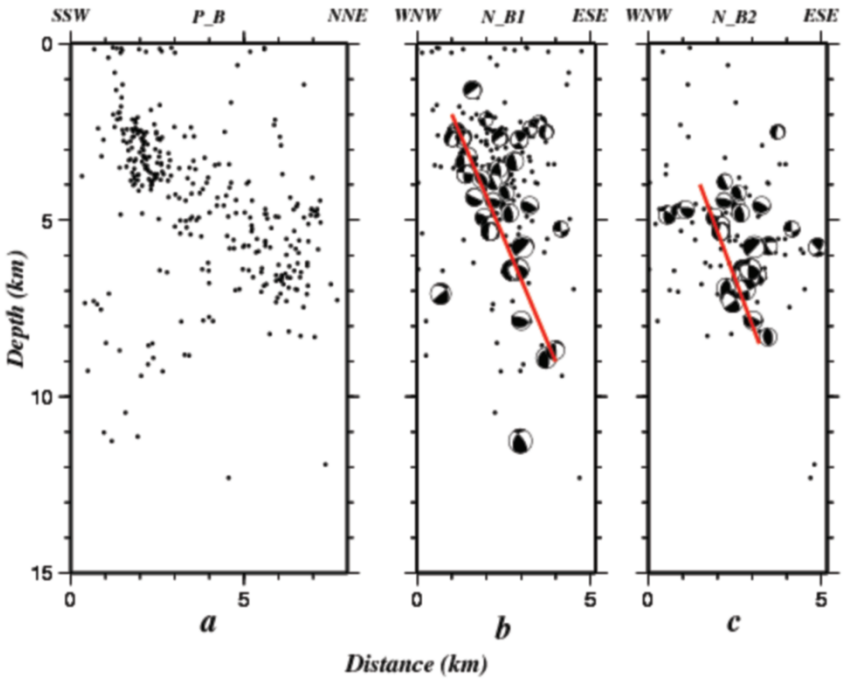

Fig. 6. Same as in Fig. 5 for the activity encompassed in the southwestern box.

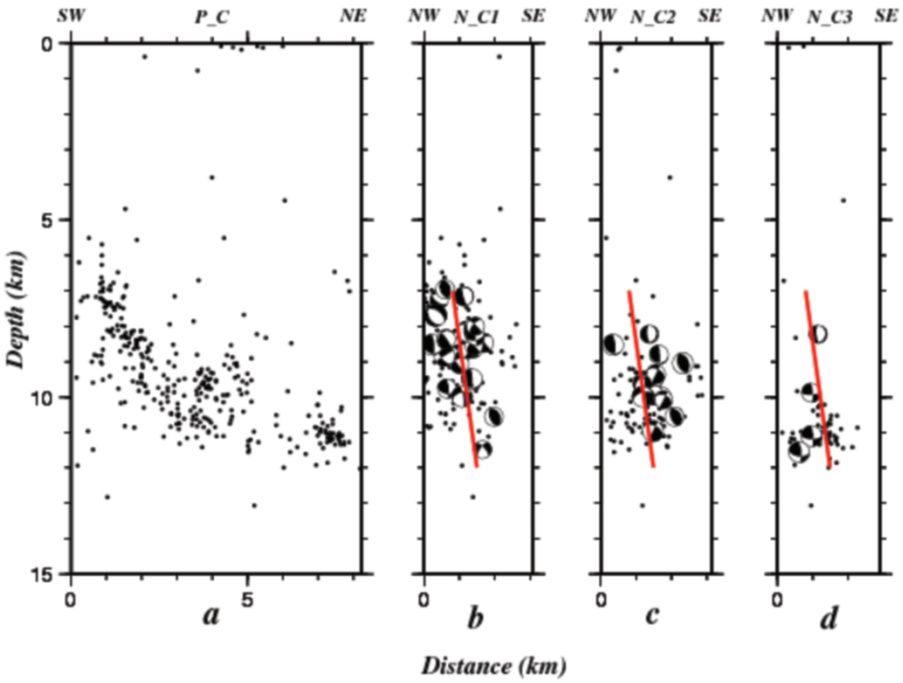

Fig. 7. Same as in Fig. 5 for the activity encompassed in the central-eastern box.

Cluster C reveals the activation of a prominent 8-km-long elongated structure in the map view (Fig. 4) that is positioned at an angle of 45° with the main rupture. From fault plane solutions of strong and moderate events that occurred along the western coastline, it means, on the Lefkada segment of CTF, the mean azimuth of P-axes is about 240° (Louvari *et al*. 1999, Benetatos *et al*. 2005). This orientation of the axis of maximum compression does not support strike slip faulting with almost the same orientation. This provides evidence for strain partitioning at this place, an observation that demands further elaboration. Figure 7a exhibits the strike parallel distribution of microseismicity which is confined between 5 and 12 km.

In the strike parallel cross section for polygon D (Fig. 8a), a rather dense distribution of off-fault aftershocks appears from 5 to 13 km depth, which is probably associated with tiny secondary faults next to the main rupture. This activity most probably reflects the deformation of the hanging wall.

Strike-normal cross sections

Karakostas (2008) has performed seven strike-normal cross sections, taking into consideration all aftershocks as one data set. We choose, instead in this study, to accomplish the respective sections normal to the strike of the four

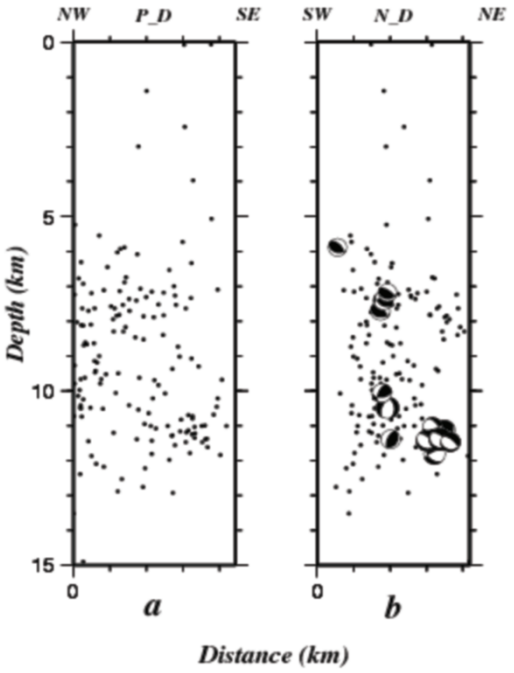

Fig. 8. Same as in Fig. 5 for the activity encompassed in the north -eastern box.

discrete clusters. The focal mechanisms of the microearthquakes are also included in these cross sections.

The three normal cross sections shown in Fig. 5b-d are in rapport between them, detailing the characteristics of the main rupture. The vast majority of the determined fault plane solutions support the strike slip nature of the causative fault, and their frontal projections, along with the vertical distribution of aftershocks foci, further support the dip of the centroid moment tensor solution determined for the main shock.

The two cross-normal sections in Fig. 6b, c manifest that the events composing cluster B are associated with a rather steep strike slip faulting, alike the main rupture. This provides further support to the possible triggering of this along strike fault segment by stress transfer from the main shock (Karakostas *et al*. 2004).

A steep fault with a designated NE-SW strike is revealed from the three normal cross sections for cluster C (Fig. 7b-d). The principal compressional stress has a mean NW-SE trend, holding the dextral strike slip nature of the activated structure, although it evidences a rotation from the dominant regional WSW-ENE trend.

The normal cross section for cluster D exhibits an interspersion of the microearthquake foci (Fig. 8b), which inhibits the feasibility for the recognition of an independent secondary fault. This fact along with the alteration of

the faulting mechanisms with depth, leads to the speculation of ascribing this activity to the deformation of a hanging wall.

In addition to the faulting characteristics identified from the 2003 aftershock activity, it is worth to mention here that at the junction of the main rupture and cluster C, the focal mechanisms exhibit NW-SE striking faults. This strike is in accordance with onshore local morphology, most probably of tectonic origin. Most importantly, this strike is in full agreement with epicentral alignment of the 1994 aftershock sequence (Fig. 9a). The *M*5.4 main shock produced extensive damage to the nearby villages. A local network was installed at that time in the area and the collected recordings (by Papaioannou and Tsapanos, personal communication) were used for the aftershock relocation. The strike normal cross section (Fig. 9b) revealed a north–eastwards dipping steep fault.

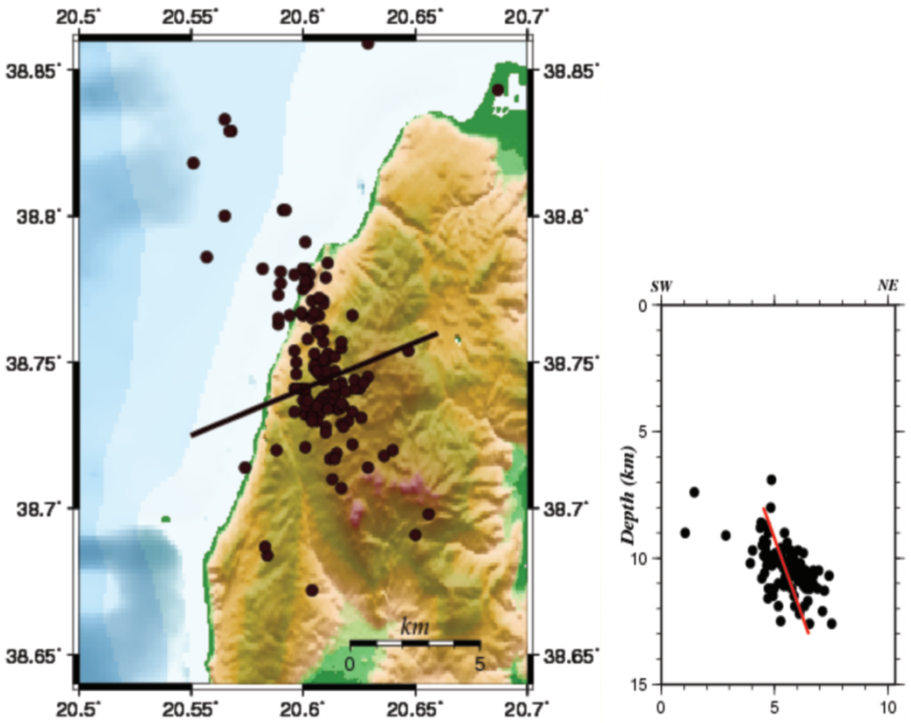

Fig. 9: (a) Spatial distribution of the 1994 aftershock sequence, implying a NW-SE striking fault plane. The thick line indicates the surface position of the plane considered for the strike normal cross section. (b) Depth cross section taken normal to the strike of the alignment of the 1994 aftershocks spatial distribution, which reveals a NE dipping fault plane. Colour version of this figure is available in electronic edition only.

5. DISCUSSION

The 2003 Lefkada earthquake reemphasized the seismic hazard of the fault zone that runs along the western coastline. This was the first strong event that occurred in modern instrumental era, although the same segment has failed again in 1914 and 1948. The wealth of aftershock data gave the means to investigate in more details the characteristics of the activity triggered and following the main event. The spatial distribution of aftershocks illuminates structures previously unknown. This means that, in addition to the slip on the main rupture, short secondary nearby faults may fail almost contemporaneously. These fairly smaller ruptures cause additional damage in areas that oftentimes cannot be explained by the ground motion assigned directly to the main rupture. Thus, unfolding the complex nature of an activated area can shed more light in faulting mechanism and in seismic hazard evaluation approach.

The complex aftershock distribution exhibits several distinctive features. First, the steeply southeast dipping zone of aftershocks is consistent with the focal mechanism of the main shock. Second, the hanging wall deformation appears to be associated with intense activity on the northeastern part of the activated area. Third, the southwestern cluster, which is markedly more superficial than the other activity, is associated with triggered activation of the adjacent fault segment that has mainly the same kinematic characteristics with the main fault, although motion on NW-SE striking planes is hinted by some fault plane solutions. Fourth, the distribution of aftershocks along a narrow band at the central eastern part of the activated area revealed the activation of a small also right-lateral strike-slip fault, which is possibly kinematically related with the main fault. However, the principal stress axes on this secondary fault appear to have been rotated significantly from the dominant regional trend. The determined fault plane solutions evidence a mechanism diversity of ~40°, which is adequately above the formal error (~20°) and adequate to disclose slip partitioning.

This is commonly observed in analogous cases, like in southern California where significant spatial heterogeneity was identified, which in some cases appeared to be a result of the complexity of faulting and in other cases appears to be a cause (Hardebeck and Hauksson 2001). Faulting complexity may not be simply the response of a heterogeneous crust to a homogeneous stress field. On the other hand, stress field heterogeneity can be related to fault complexity, such as stepovers and junctions. Complex faulting may promote heterogeneous stress field and *vice versa*. From the above and our results, it seems likely that the orientations of the secondary structures would control the aftershock focal mechanisms, rather than just the orientation of the regional stress field.

The inferred slip partitioning postulates that future moderate-size earthquakes may be caused by faults with different orientation and location than the main fault system which was up to now known for the Island of Lefkada. The occurrence of even smaller magnitude events that can radiate damaging ground motions thus need to be included in seismic hazard assessment studies. The length of the activated secondary eastern fault is most probably structurally controlled, although it cannot be firmly established. Nevertheless, it can well sustain an earthquake of $M \sim 5.5$ if it slips entirely. Moderate events occur often in the study area, some of them inland, causing appreciable damage and thus posing an additional hazard to the one coming from the main fault system. Then, the identification of these subsidiary faults and their properties contributes significantly to the future seismic hazard assessment.

Acknowledgments. This work was partially supported by the Local Union of Lefkada Island Municipalities. The provision of the recordings of the 1994 aftershock sequence by C. Papaioannou and T. Tsapanos is greatly appreciated. The GMT system (Wessel and Smith 1998) was used to plot the figures. The paper is benefited by thorough revisions from Haluk Eyidogan and an anonymous reviewer. Geophysics Department contribution 749.

References

Benetatos, C., A. Kiratzi, Z. Roumelioti, G. Stavrakakis, G. Drakatos, and I. Latoussakis (2005), The 14 August 2003 Lefkada Island (Greece) earthquake: Focal mechanisms of the mainshock and of the aftershock sequence, *J. Seismology* **9**, 2, 171-190, DOI: 10.1007/s10950-005-7092-1.

Benetatos, C., D. Dreger, and A. Kiratzi (2007), Complex and segmented rupture associated with the 14 August 2003 M_w6.2 Lefkada, Ionian Islands, earthquake, *Bull. Seism. Soc. Am.* **97**, 1B, 35-51, DOI: 10.1785/0120060123.

Hardebeck, J.L., and E. Hauksson (2001), Crustal stress field in southern California and its implications for fault mechanics, *J. Geophys. Res.* **106**, B10, 21,859-21,882, DOI: 10.1029/2001JB000292.

Hatzfeld, D., V. Karakostas, M. Ziazia, G. Selvaggi, S. Leborgne, C. Berge, R. Guiguet, A. Paul, P. Voidomatis, D. Diagnourtas, I. Kassaras, I. Koutsikos, K. Makropoulos, R. Azzara, M. Di Bona, S. Baccheschi, P. Bernard, and C. Papaioannou (1997), The Kozani–Grevena (Greece) earthquake of 13 May 1995 revisited from a detailed seismological study, *Bull. Seism. Soc. Am.* **87**, 2, 463-473.

Karakostas, V. (2008). Relocation of aftershocks of the 2003 Lefkada Sequence: seismotectonic implications, *Proc. 3rd Hellenic Conf. Earthq. Engin. & Engin. Seism., Athens, 5-7 Nov. 2008*, CD ROM, 16 pp.

Karakostas, V.G., E.E. Papadimitriou, and C.B. Papazachos (2004), Properties of the 2003 Lefkada, Ionian Islands, Greece, earthquake seismic sequence and seismicity triggering, *Bull. Seism. Soc. Am.* **94**, 5, 1976-1981, DOI: 10.1785/012003254.

Kiratzi, A.A., and C.A. Langston (1991), Moment tensor inversion of the 1983 January 17 Kefallinia event of Ionian islands (Greece), *Geophys. J. Int.* **105**, 2, 529-535, DOI: 10.1111/j.1365-246X.1991.tb06731.x.

Klein, F.W. (2002), User's Guide to HYPOINVERSE-2000, a Fortran program to solve earthquake locations and magnitudes, U. S. Geol. Surv. Open File Report 02-171, Version 1.0.

Louvari, E., A.A. Kiratzi, and B.C. Papazachos (1999), The Cephalonia Transform Fault and its extension to western Lefkada Island (Greece), *Tectonophysics* **308**, 1-2, 223-236, DOI: 10.1016/S0040-1951(99)00078-5.

Papadimitriou, E.E. (1993), Focal mechanism along the convex side of the Hellenic Arc, *Boll. Geof. Teor. Appl.* **35**, 401-426.

Papadimitriou, E.E. (2002), Mode of strong earthquake recurrence in the central Ionian Islands (Greece): Possible triggering due to Coulomb stress changes generated by the occurrence of previous strong shocks, *Bull. Seismol. Soc. Am.* **92**, 8, 3293-3308, DOI: 10.1785/0120000290.

Papadimitriou, P., G. Kaviris, and K. Makropoulos (2006), The $M_w = 6.3$ 2003 Lefkada earthquake (Greece) and induced stress transfer changes, *Tectonophysics* **423**, 1-4, 73-82, DOI: 10.1016/j.tecto.2006.03.003.

Papadopoulos, G.A., V.K. Karastathis, A. Ganas, S. Pavlides, A. Fokaefs, and K. Orfanogiannaki (2003), The Lefkada, Ionian Sea (Greece), shock (M_w6.2) of 14 August 2003: Evidence for the characteristic earthquake from seismicity and ground failures, *Earth Planets Space* **55**, 713-718.

Papathanassiou, G., S. Pavlides, and A. Ganas (2005), The 2003 Lefkada earthquake: Field observations and preliminary microzonation map based on liquefaction potential index for the town of Lefkada, *Eng. Geol.* **82**, 1, 12-31, DOI: 10.1016/j.enggeo.2005.08.006.

Papazachos, B.C., and P.E. Comninakis (1971), Geophysical and tectonic features of the Aegean Arc, *J. Geophys. Res.* **76**, 35, 8517-8533, DOI: 10.1029/JB076i035p08517.

Papazachos, B.C., and C.B. Papazachou (2003), *The Earthquakes of Greece*, Ziti Publications, Thessaloniki, 286 pp.

Papazachos, B.C., E.E. Papadimitriou, A.A. Kiratzi, C.B. Papazachou, and E.K. Louvari (1998), Fault plane solutions in the Aegean sea and the surrounding area and their tectonic implication, *Boll. Geof. Teor. Appl.* **39**, 3, 199-218.

Reasenberg, P., and D. Oppenheimer (1985), FPFIT, FPPLOT and FPPAGE: FORTRAN computer programs for calculating and displaying earthquake fault-plane solutions, U.S. Geol. Surv. Open File Rep. 109, 85-730.

Scordilis, E.M., G.F. Karakaisis, B.G. Karakostas, D.G. Panagiotopoulos, P.E. Comninakis, and B.C. Papazachos (1985), Evidence for transform faulting in the Ionian sea: The Cephalonia island earthquake sequence of 1983, *Pure Appl. Geophys.* **123**, 3, 388-397, DOI: 10.1007/BF00880738.

Wessel, P., and W.H.F. Smith (1998), New, improved version of generic mapping tools released, *Eos Trans. AGU* **79**, 47, 579, DOI: 10.1029/98EO00426.

Zahradník, J., A. Serpetsidaki, E. Sokos, and A. Tselentis (2005), Iterative deconvolution of regional waveforms and a double-event interpretation of the 2003 Lefkada earthquake, Greece, *Bull. Seism. Soc. Am.* **95**, 1 159-172, DOI: 10.1785/0120040035.

Received 13 July 2009
Accepted 23 September 2009